



# SPP1 mRNA determination based on molecular beacon for the recurrence prognosis of bladder cancer

Zhouliang Wu<sup>1,2#</sup>, Donghuai Wang<sup>1,2#</sup>, Yu Zhang<sup>1,2#</sup>, Zhe Zhang<sup>1,2</sup>, Chong Shen<sup>1,2</sup>, Zhongcheng Xin<sup>1,2</sup>, Yuhong Feng<sup>1,2</sup>, Hailong Hu<sup>1,2</sup>

<sup>1</sup>Department of Urology, The Second Hospital of Tianjin Medical University, Tianjin, China; <sup>2</sup>Tianjin Key Laboratory of Urology, Tianjin Institute of Urology, The Second Hospital of Tianjin Medical University, Tianjin, China

**Contributions:** (I) Conception and design: Z Wu, D Wang, Y Zhang; (II) Administrative support: H Hu, Z Xin; (III) Provision of study materials or patients: H Hu, Y Feng; (IV) Collection and assembly of data: D Wang, Y Zhang; (V) Data analysis and interpretation: Z Wu, D Wang; (VI) Manuscript writing: All authors; (VII) Final approval of manuscript: All authors.

<sup>#</sup>These authors contributed equally to this work.

**Correspondence to:** Hailong Hu, PhD; Yuhong Feng, MD. Department of Urology, The Second Hospital of Tianjin Medical University, Tianjin 300211, China; Tianjin Key Laboratory of Urology, Tianjin Institute of Urology, The Second Hospital of Tianjin Medical University, Pingjiang Road 23, Tianjin 300211, China. Email: huhailong@tmu.edu.cn; mnwkfyh@163.com.

**Background:** Bladder cancer (BC) has attracted significant attention on account of its recurrence as well as mortality. Tumor recurrence plays a significant role in cancer patients' individual treatment. Secreted phosphoprotein 1 (SPP1) has been recognized as a potential target for treating BC and served as a useful biomarker for prognosis; it is commonly tested by immunohistochemistry (IHC). However, this conventional method has the disadvantage of being time-consuming and costly. This study aimed to develop a molecular beacon (MB) for the detection of SPP1 messenger RNA (mRNA) for the recurrence prognosis of BC.

**Methods:** An MB was constructed and applied to image SPP1 mRNA level at both molecular and cellular level. The fluorescence spectra were recorded with a fluorescence spectrophotometer. The effect of SPP1 MB toward the cell viability was performed by Cell Counting Kit-8 (CCK-8) assays. The SPP1 mRNA expression level was measured by quantitative real-time polymerase chain reaction (qRT-PCR). Cancer cells and tissues were analyzed with confocal fluorescence imaging. Correlation, sensitivity, and specificity parameters were calculated.

**Results:** It was demonstrated that both cancer cells and BC tissues expressed high signal which reflected the expression of SPP1. In addition, 42 cases were detected by MB and divided into two groups according to the fluorescence intensity. The results further suggested that highly expressed SPP1 could predict early tumor recurrence in BC.

**Conclusions:** The SPP1 MB could be applied as an appropriate approach to predict BC recurrence and patients' prognosis.

**Keywords:** Secreted phosphoprotein 1 (SPP1); molecular beacon (MB); messenger RNA (mRNA); bladder cancer (BC)

Submitted Aug 17, 2023. Accepted for publication Nov 29, 2023. Published online Dec 15, 2023.

doi: 10.21037/tau-23-432

View this article at: <https://dx.doi.org/10.21037/tau-23-432>

## Introduction

Bladder cancer (BC) is the sixth most frequently diagnosed cancer and the second most prevalent urologic malignancy in men (1-3). A wide variety of treatment for BC including

radical cystectomy (4), bladder-sparing therapy with transurethral resection (5), chemotherapy (6), radiotherapy (7), and immunotherapy (8) has been applied. However, the prognosis is poor with a survival rate of 30–50% for

patients with deeply invasive BC (9). In addition, common characteristics of patients with BC are high rates of recurrence as well as metastasis (10). Therefore, prognosis is crucial for clinical decision making and individualized treatment of patients with BC.

Secreted phosphoprotein 1 (SPP1) is an acidic arginine-glycine-aspartate containing adhesive glycoprotein (11,12) which is secreted by different types of cells. Recently, SPP1 has been reported to play crucial roles in tumor growth and metastasis including cell proliferation, adherence, and invasion (13,14). Furthermore, over expression of SPP1 has been found in bladder (15), prostate (16), breast (17), colon (18), and lung cancers (19). Besides, the SPP1 expression level in cancer is related to tumor stage and aggressiveness (20). Ahmed *et al.* reported that SPP1 secreted by macrophages could combine with CD44s on the surface of cancer cells (11). Sjö Dahl *et al.* reported that SPP1 expression could predict the efficacy of cisplatin-based neoadjuvant chemotherapy in certain patients (21). In view of this, SPP1 plays significant role in promoting invasion and growth. Therefore, SPP1 could serve as a biomarker for diagnosis as well as prognosis in a series of cancers.

A lot of assays involving northern blot (NB) (22,23),

in situ hybridization (ISH) (24,25), and polymerase chain reaction (PCR) (26) have been proposed to detect endogenous messenger RAN (mRNA). The lung cancer PDCD4 mRNA has been determined by Zhen *et al.* via NB assay (27). ISH-technologies have been applied to analyze the level of KRAS mRNA in tissue (28). Kurrasch *et al.* have developed a method for the measurement of the content of G-protein signaling mRNA by PCR (29). Nevertheless, these methods mentioned above have several drawbacks including relatively time-consuming procedure, large sample consumption, and low sensitivity.

The fluorescent method has attracted great attention because of its relatively high sensitivity, low cost, appropriate selectivity, and convenience (30-35). In these systems, molecular beacon (MB) is applied to monitor the expression of nucleic acid in living cells (36-38). MB consists of three units: a fluorophore, a quencher, and a single-strand DNA. Both the fluorophore and quencher elements comprise a signaling unit. A single-strand DNA with loop-stem hairpin structure acts as a recognition unit. A weak signal is observed in the absence of a target owing to fluorescence resonance energy transfer between the fluorophore and quencher. The quencher of the probe endows its low background. Upon addition of a target, bright fluorescence can be observed after conformational transition. Consequently, the target could be determined in a single-step process. In addition, no reverse transcription nor other helper strand are needed in the MB probe, thus reducing detection steps and gaining time. A series of fluorescence probes have been reported on regarding their capability in detecting the content of RNA including ribosomal RNA (rRNA) (39), mRNA (28), microRNA (miRNA) (40), and long non-coding RNA (lncRNA) (41), and have been used for diagnosis, prognosis, and identification of the tumor progression. Thus, the MB probe is a crucial tool to detect SPP1 mRNA for the prognostic assessment of the tumors.

In this work, a fluorescence probe based on MB was proposed for the determination of SPP1 in both BC cells and tissues. The conformational transition in this fluorescence probe was induced with the presence of SPP1 mRNA, the loop was opened, and a bright green fluorescence was observed. Moreover, the SPP1 probe could be employed to provide important information for the prediction in terms of the recurrence of BC. Therefore, this proposed approach provided a platform to detect SPP1, demonstrating crucial potential in prognostic judgment of BC patients based on SPP1-related gene expression. We present this article in accordance with the MDAR reporting

### Highlight box

#### Key finding

- We have developed a molecular beacon (MB) to detect the secreted phosphoprotein 1 (SPP1) messenger RNA (mRNA) with high sensitivity and selectivity both in cells and tissues. The present study suggests that SPP1 MB could be applied as an appropriate approach to predict bladder cancer (BC) recurrence and patient prognosis.

#### What is known and what is new?

- SPP1 has been reported to play crucial roles in tumor growth and metastasis including cell proliferation, adherence, and invasion. SPP1 expression could predict the efficacy of cisplatin-based neoadjuvant chemotherapy in certain patients. However, the majority of previous research has been driven towards immunohistochemical expression of SPP1.
- Here, we develop an MB for the detection of SPP1 mRNA for the recurrence prognosis of BC.

#### What is the implication, and what should change now?

- SPP1 MB could be applied as an appropriate approach to predict BC recurrence and patients' prognosis according to the fluorescence signal.
- Future research may include larger sample sizes from more medical centers.

checklist (available at <https://tau.amegroups.com/article/view/10.21037/tau-23-432/rc>).

## Methods

### Reagents

Cell Counting Kit-8 (CCK-8) was obtained from Solarbio Science & Technology Co., Ltd. (Beijing, China) Primary antibody against SPP1 was purchased from Abcam Inc. (ab214050; Cambridge, MA, USA). Unless otherwise stated, no further purification was required for other reagents and chemicals purchased from Sigma-Aldrich (St. Louis, MO, USA).

DNA sequences designed in this work (Table S1) were provided by Sangon Biotech (Shanghai, China).

### Instruments

The fluorescence spectra were recorded using a Hitachi F-4500 fluorescence spectrophotometer. Microplate reader (Infinite M200 PRO; Tecan Life Sciences, Grödig, Austria) was used to measure the absorbance of CCK-8. Confocal laser scanning microscopy images were collected using confocal laser scanning microscope (CLSM; LSM 710; Zeiss, Oberkochen, Germany).

### Cells culture

T24 cells were obtained from American Type Culture Collection (ATCC; Manassas, VA, USA) and then were maintained by Dulbecco's modified Eagle medium (DMEM) containing 10% fetal bovine serum (FBS) and 1% penicillin/streptomycin. T24 cells were incubated in a humidified incubator at 37 °C containing 5% CO<sub>2</sub>. Before the experiment, cell density was quantified by a hemocytometer.

### Cytotoxicity assay

The effect of SPP1 MB toward the cell viability was demonstrated by CCK-8 assays. T24 cells at a density of  $5 \times 10^3$ /mL cells were plated in 96-well plates and incubated overnight. Subsequently, the cells were incubated with different concentrations of SPP1 MB (0–10 μM). After 24 hours, CCK-8 solution (20 μL) was added into 96-well plates incubated for 1 hour in a humidified incubator. The absorbance of CCK-8 at 450 nm was measured by microplate reader.

### Confocal fluorescence imaging

A total of  $4 \times 10^4$  T24 cells were inoculated in a 35 mm glass-bottom dish and cultivated for 24 hours. The T24 cells were washed in phosphate-buffered saline (PBS; 0.1 M, pH 7.4) thrice and left in fresh Opti-MEM. After 2 hours, 6 μL Lipofectamine 3000 reagent (Thermo Fisher, Waltham, MA, USA), or 8.4 μL 100 μM SPP1 MB was added into a 1.5 mL tube, and then 140 μL Opti-MEM were added and was left for 5 minutes at room temperature. Thereafter, the above two solutions were mixed and allowed to stand for 20 minutes. The mixture solution was added into glass-bottom dish for 4 hours. Cells were washed with PBS thrice and were added to 1 mL PBS prior to confocal imaging. The T24 cells were observed by laser confocal microscope (Zeiss LSM 710) with a 40× objective. The images were captured with appropriate excitation for 4',6-diamidino-2-phenylindole (DAPI; 405 nm) and SPP1 MB (488 nm).

### Quantitative real-time PCR (qRT-PCR) analysis, clinical sample analysis, and immunohistochemistry (IHC)

The detailed process is described in Appendix 1.

### Human biological samples

The tissue samples were collected from the Second Hospital of Tianjin Medical University (Tianjin, China). The study was conducted in accordance with the Declaration of Helsinki (as revised in 2013). The study was approved by the Tianjin Medical University Management Committee and Ethics Committee (No. KY2021K113) and the requirement for individual consent for this retrospective analysis was waived.

### Statistical analysis

An unpaired *t*-test using GraphPad Prism 8.0 (GraphPad Software, San Diego, CA, USA) with Welch's correction was used to assess the endpoints. All statistical tests were two-tailed and a *P* value <0.05 was considered significant.

## Results

### The design and feasibility of MB for the determination of SPP1 mRNA

We successfully designed and synthesized the special MB which composed of 3 units: single-strand DNA, a

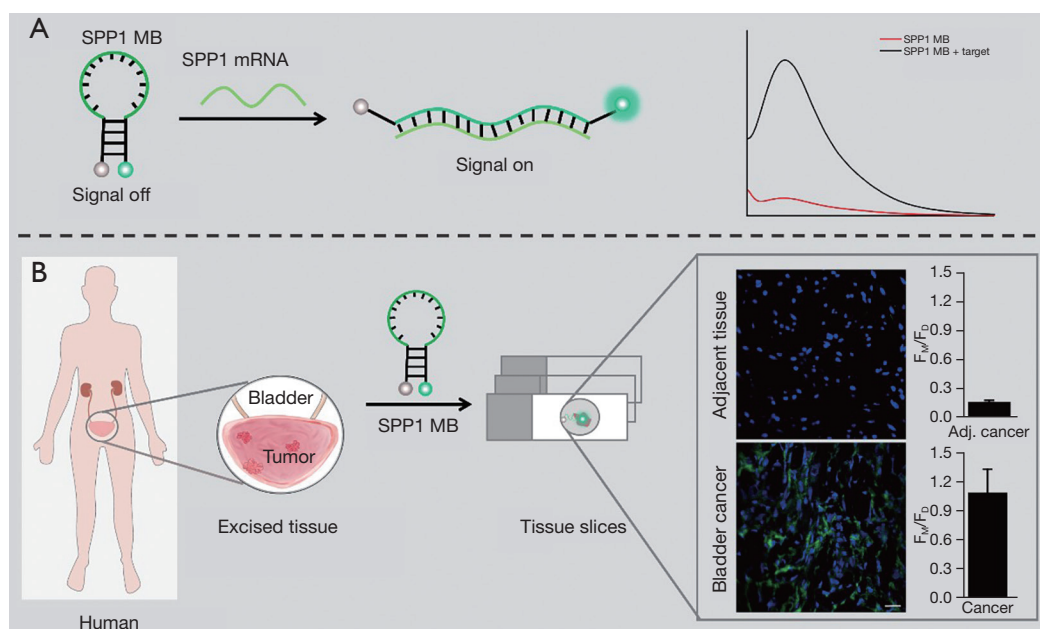


**Figure 1** The design of the MB and its detection process. (A) Schematic illustration of the design of MB for the determination of SPP1 mRNA. (B) Schematic illustration of MB for the detection of SPP1 mRNA in tissue. SPP1, secreted phosphoprotein 1; MB, molecular beacon; mRNA, messenger RNA; adj., adjacent.

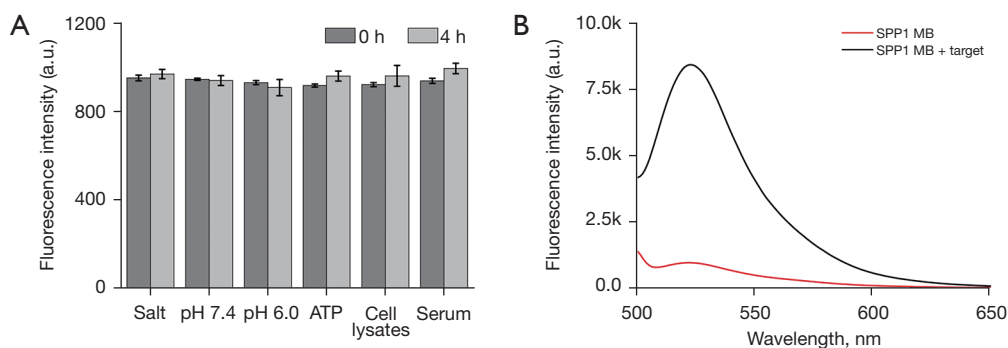


**Figure 2** The feasibility of target gene detection. (A) The relative fluorescence intensity of SPP1 MB in the presence of salt (20 mM Tris-HCl, 150 mM NaCl, and 5 mM MgCl<sub>2</sub>), pH=7.4, pH=6.0, ATP (2 mM), cell lysates and serum for 4 h. (B) Fluorescence spectra to confirm the feasibility of the SPP1 MB for the detection of SPP1 mRNA. SPP1 MB (6 μM) was incubated in the presence or absence of target at 37 °C for 4 h. a.u., arbitrary units; ATP, adenosine 5'-triphosphate; SPP1, secreted phosphoprotein 1; MB, molecular beacon; mRNA, messenger RNA.

fluorophore (FAM), and a quencher (Dabcyl). The specific structure and detailed workflow are shown in *Figure 1*. Further, it was found that this designed probe could be employed to analyze the expression of SPP1 mRNA in a biological environment. As shown in *Figure 2A*, the fluorescence was weak in various solutions. However, the signal of hairpin (curve black) increased 8.57 folds in the

presence of target, demonstrating that SPP1 mRNA could hybridize with hairpin (*Figure 2B*).

#### *In vitro and vivo response and specificity of SPP1 MB*

After verification, the feasibility of the probe design was demonstrated to be capable of target concentration

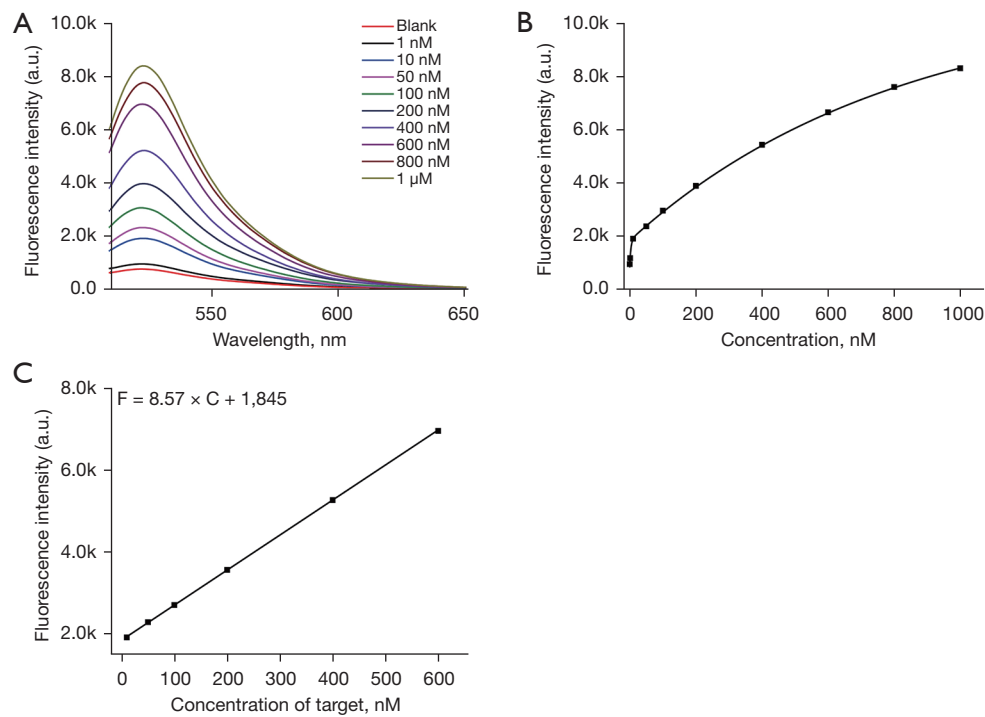


**Figure 3** *In vitro* response of SPP1 MB. (A) Fluorescence spectra of SPP1 MB treatment with various concentrations of DNA target (0–1 μM). (B) Relationship between the fluorescence intensity of SPP1 MB and the DNA target concentration. (C) The linear relationship between relative fluorescence intensity of SPP1 MB and DNA target concentration. a.u., arbitrary units; SPP1, secreted phosphoprotein 1; MB, molecular beacon.

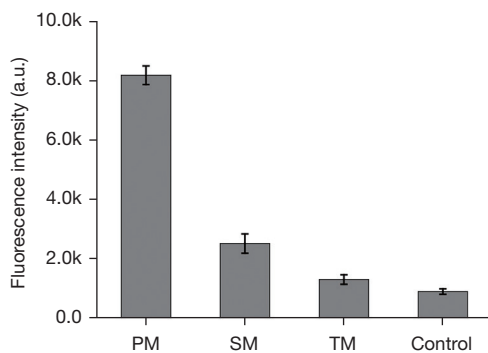


**Figure 4** Specificity evaluation of the SPP1 MB for the determination of SPP1 mRNA. PM, SM, TM, (n=3). a.u., arbitrary units; PM, perfect match; SM, single-base mismatched strand; TM, three-base mismatched strand; SPP1, secreted phosphoprotein 1; MB, molecular beacon; mRNA, messenger RNA.

determination (Figure 3A,3B). The nonlinear relationship between the signal and concentration of target range from 10 nM to 1 μM was obtained. The fluorescence signal versus the content of target demonstrated a good relationship

ranging of 10–600 nM (Figure 3C). Even though at the lowest levels (10 nM), detectable fluorescence signals were observed. Subsequently, we assessed the specificity of SPP1 MB. As displayed in Figure 4, strong fluorescence intensity was observed in the MB-treated target analyte.

*In vivo* studies have found that the probe exhibits no overt toxicity toward T24 cells even with the MB up to 10 μM (Figure 5A). When the concentration of SPP1 mRNA changes in living cells, the MB can accurately react to the corresponding cellular environment (Figure 5B–5E).

#### **Human tissues imaging and clinical prognosis based on the fluorescence signal of SPP1 MB**

The SPP1 MB was successfully applied to determine the SPP1 mRNA level in the BC and adjacent normal tissues (Figure 6A–6D). The results above were in good agreement with the results obtained from conventional IHC staining (Figure 7) and qRT-PCR (Figure S1). Furthermore, the SPP1 highly expressed group demonstrated a comparatively high risk of recurrence (Figure S1, Figure 8).

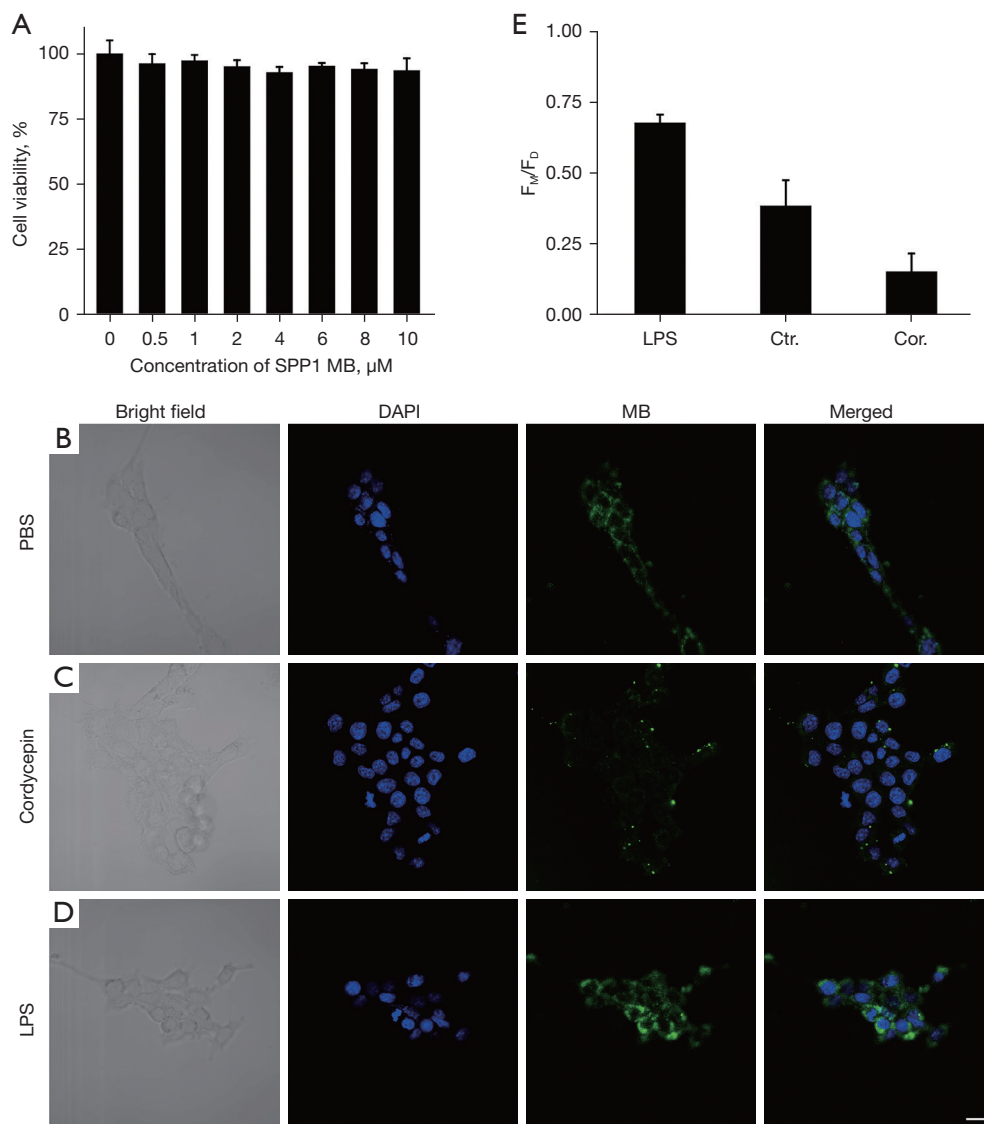


**Figure 5** Intracellular detection of SPP1 mRNA using SPP1 MB. (A) Cytotoxicity of SPP1 MB toward T24 cells after treated with varying concentration of T24 SPP1 MB of various concentration ranging from 0–10  $\mu\text{M}$  for 24 h. CLSM images of mRNA in T24 cells under different conditions. Cells were pretreated with (B) PBS, (C) Cor., and (D) LPS for 2 h. Detailed process was described in materials and methods (2.5). (E) The relative fluorescence intensity of Cor., Ctr., and LPS ( $n=3$ ). Scale bar: 20  $\mu\text{m}$ . SPP1, secreted phosphoprotein 1; MB, molecular beacon; LPS, lipopolysaccharide; Ctr., control, PBS; PBS, phosphate-buffered saline; Cor., cordycepin; DAPI, 4',6-diamidino-2-phenylindole; mRNA, messenger RNA; CLSM, confocal laser scanning microscope.

## Discussion

### *Working principle of MB for the determination of SPP1 mRNA*

The strategy for the determination of SPP1 mRNA is shown in *Figure 1*. The SPP1 MB was composed of three units: single-strand DNA, FAM, and Dabcyl, respectively.

FAM was the fluorophore with green emissive, whereas Dabcyl was the quencher which was used to quench the fluorescence of FAM. The single-strand consists of two elements: the loop of DNA served as a recognition element which is complementary to SPP1 mRNA, whereas the stem of DNA which could hybridize each other. Both FAM and Dabcyl were employed as a signal unit. MB was capable of

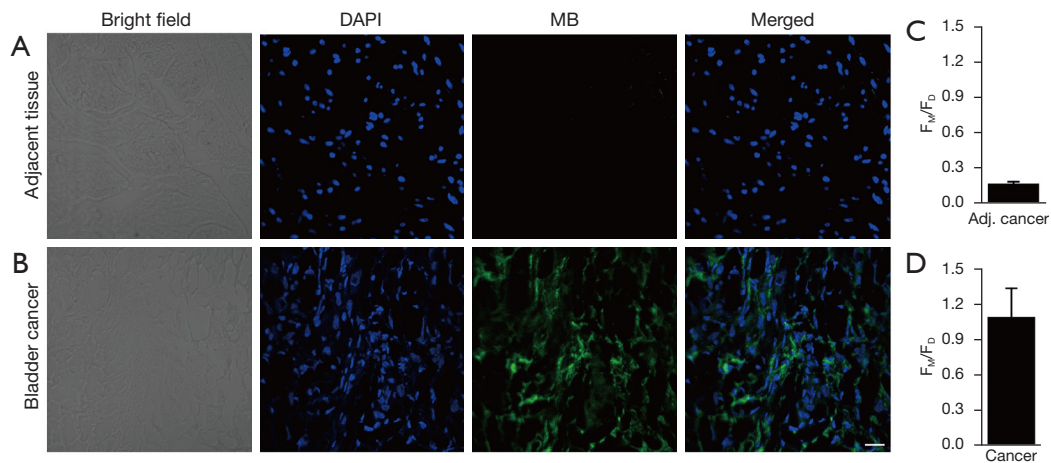


**Figure 6** CLSM images of (A) BC adjacent tissue (adj. cancer) and (B) BC treated with SPP1 MB. Human BC tissues were fixed by formalin before experiment. The slides were treated with 100  $\mu$ L 6  $\mu$ M SPP1 MB for 4 h at 37  $^{\circ}$ C. Subsequently, the slides were washed 3 times with PBS and were examined by laser confocal microscope (Zeiss LSM 710 with a 40 $\times$  objective). The relative fluorescence intensity of (C) adjacent tissue and (D) BC. Scale bar: 20  $\mu$ m. DAPI, 4',6-diamidino-2-phenylindole; MB, molecular beacon; adj., adjacent; CLSM, confocal laser scanning microscope; BC, bladder cancer; SPP1, secreted phosphoprotein 1; PBS, phosphate-buffered saline.

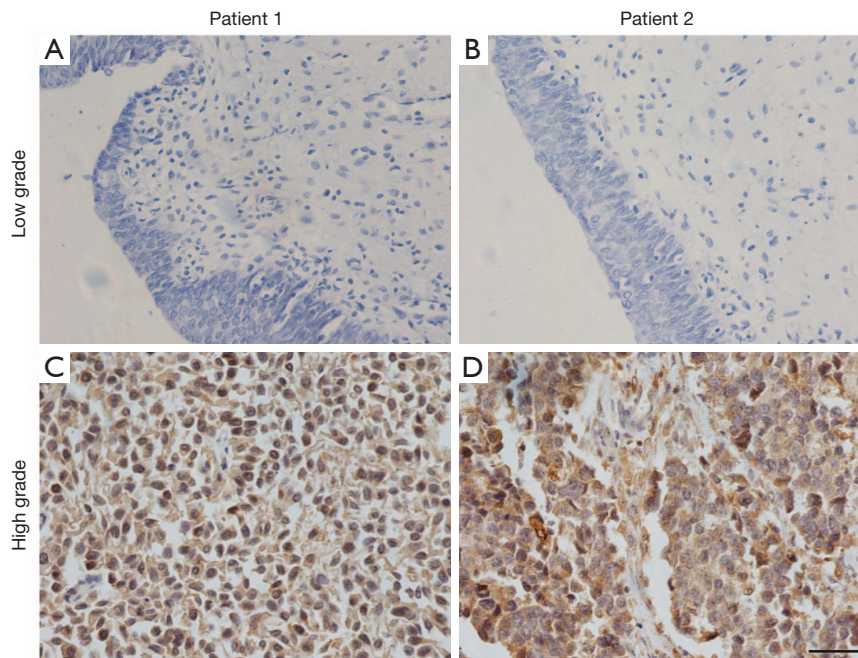


**Figure 7** IHC staining for SPP1 in the (A,B) cancer adjacent tissue and (C,D) tumor tissue of patients. Scale bar: 50  $\mu$ m. IHC, immunohistochemistry; SPP1, secreted phosphoprotein 1.

hybridizing with target to form a double strand, resulting in the conformational change of probe. As a result, the distance between the fluorophore and quencher increased accompanied with disruption of Forster resonance energy

transfer (FRET), leading to bright fluorescence. The signal intensity of FAM which was detected at 520 nm was capable of employing as a signal for the determination of SPP1 mRNA. Furthermore, the probe could be employed

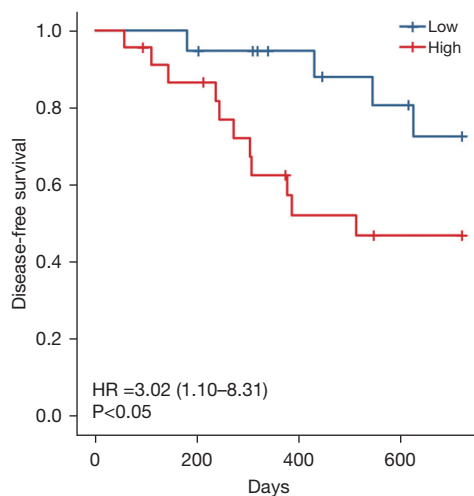


**Figure 8** Kaplan-Meier recurrence of BC based on the results of SPP1 MB signal. HR, hazard ratio; BC, bladder cancer; SPP1, secreted phosphoprotein 1; MB, molecular beacon.

to detect the SPP1 mRNA expression in tumors for BC prognosis.

#### **Feasibility of target gene detection**

The stability of MB was first investigated via fluorescence spectra before practical application, then we carried an experiment that mimics physiologic conditions. As shown in *Figure 2A*, the fluorescence was weak in various solutions. Then, the probe was subjected in physiologic conditions for 2 hours, and very minor change of the fluorescence signal was observed demonstrating relative high stability in physiologic conditions. The signal of hairpin (curve black) increased 8.57 folds in the presence of a target, demonstrating that SPP1 mRNA could hybridize with hairpin (*Figure 2B*). On the contrary, no significant changes in the fluorescent signal (curve red) were visualized without a target, indicating that no reaction occurred. These results suggested that this designed probe could be employed to analyze the expression of SPP1 mRNA in a biological environment.

#### **In vitro response of SPP1 MB**

After verification, the feasibility of the constructed probe was demonstrated to be able to determine the concentration of target. Subsequently, the *in vitro* studies for SPP1 mRNA detection through the probe were performed by

fluorescence spectra and polyacrylamide gel electrophoresis (PAGE). The fluorescence recovery effect was evaluated through adding varied concentrations of analyte into the SPP1 MB. In the presence of analyte, the signal (*Figure 3A*) gradually increased with the target ranging from 10 nM to 1  $\mu$ M. The maximum fluorescence intensity of MB was about 7.5 times that of SPP1 MB without analyte. As shown in *Figure 3B*, the nonlinear relationship between the signal and concentration of target in the range from 10 nM to 1  $\mu$ M was obtained. The fluorescence signal versus the content of target demonstrated a good relationship ranging from 10 to 600 nM (*Figure 3C*), the formula is  $F = 8.57 \times C + 1,845$ , with a correlation coefficient square equal to 0.9921. Since a detectable fluorescence signal could be observed at the minimum content (10 nM), the limit of hairpin towards SPP1 mRNA was 10 nM, which is comparable with that reported previously (42).

#### **Specificity of SPP1 MB**

As many similar sequences existed among the RNA family, determination of the specificity of MB toward target was essential. To do so, the SPP1 MB was incubated with single-stranded nucleic acid including target, single base mismatches, and three base mismatches at same concentration. As displayed in *Figure 4*, strong fluorescence intensity was observed in the MB-treated target analyte. For the one-base mismatched sequence, slight enhancement of fluorescence intensity was observed. The change of the signal was low after treatment with three base mismatches. Therefore, only a target could induce a significant fluorescent signal, whereas not only one-base mismatch but also three-base mismatch yielded small interference for SPP1 mRNA determination. Thus, the above results demonstrated that the SPP1 MB was capable of detecting SPP1 mRNA with high specificity.

#### **Intracellular detection of SPP1 mRNA using SPP1 MB**

The MB could be employed to determine mRNA *in vitro*. Before the detection of SPP1 mRNA expression by MB, the cytotoxicity of MB was examined by utilizing CCK-8 assay. The probe exhibits no overt toxicity toward T24 cells even the MB up to 10  $\mu$ M (*Figure 5A*). *Figure 5B* shows the confocal laser fluorescence images of T24 cells after incubation with SPP1 MB at 37  $^{\circ}$ C for 2 hours. Obvious fluorescence was observed in cancer cells, demonstrating that MB could efficiently enter into cells. In addition, the

cell was pretreated with cordycepin to decrease mRNA expression. As displayed in *Figure 5C*, the fluorescence decreased in comparison to that of the untreated cells. For further imaging the SPP1 content in cancer cells, the SPP1 mRNA expression in cancer cells was increased after treatment with lipopolysaccharides (LPSs). Subsequently, a distinct signal was visualized from the cells treated with LPS (*Figure 5D*). The relative fluorescence intensity is shown in *Figure 5E*. The above results were consistent with the results of PCR after treatment with cordycepin and LPS. Thus, the fluorescence intensity in living cell was changed with the concentration of SPP1 mRNA, indicating the capability of MB to image SPP1 mRNA in living cells.

### *mRNA imaging using MB for clinical prognosis*

In view of MB having shown good biocompatibility and capability to detect SPP1 mRNA, we performed tissue imaging on samples of patients with BC. Thus, the difference in expressions of SPP1 mRNA in the BC and adjacent normal tissues were assessed. As displayed in *Figure 6A,6B*, discrepant fluorescence signals were observed and measured in adjacent normal and BC tissues after incubation with SPP1 MB, demonstrating that the latter expressed a higher SPP1 mRNA. As indicated by the fluorescence intensity analysis of these tissue slices (*Figure 6C,6D*), the fluorescence signal in BC was 1.09, which was approximately 6.8-fold more than that in adjacent tissues. The results above were in good agreement with the results obtained from IHC (*Figure 7*) and q-PCR (*Figure S1*). Furthermore, the SPP1 MB was successfully applied to determine the SPP1 mRNA level in tumor tissues. As demonstrated in *Figure S2*, BC tissues were divided into two groups according to fluorescence intensity. *Figure 8* shows that the SPP1 highly expressed group was observed to have a comparatively high risk of recurrence. Thereby, SPP1 MB is an efficient method when applied to predict BC patients' prognosis.

### **Conclusions**

In summary, SPP1 has been demonstrated as a potential therapeutic target for BC. Herein, we have developed a MB to detect the SPP1 mRNA with high sensitivity and selectivity both in cells and tissues. Compared with adjacent tissues, the BC tissues have higher expression of SPP1. Moreover, patients with a highly expressed SPP1 mRNA level are associated with early recurrence and the

fluorescence signal is inversely correlated with BC patients' prognosis. Hence, the present study suggested that SPP1 MB could be applied as an appropriate approach to predict BC recurrence and patients' prognosis.

### **Acknowledgments**

Grateful acknowledgements are made to the Second Hospital of Tianjin Medical University for the Research Platform and Jianing Guo in Department of Pathology for the Technical Guidance on Immunohistochemistry.

*Funding:* This study was supported by the Tianjin Municipal Health Industry Key Project (No. TJWJ2022XK014), the Scientific Research Project of Tianjin Municipal Education Commission (No. 2022ZD069), the Youth Fund of the Second Hospital of Tianjin Medical University (No. 2022ydey15), and the Talents Cultivated Project of Department of Urology, the Second Hospital of Tianjin Medical University (No. MNRC202313).

### **Footnote**

*Reporting Checklist:* The authors have completed the MDAR reporting checklist. Available at <https://tau.amegroups.com/article/view/10.21037/tau-23-432/rc>

*Data Sharing Statement:* Available at <https://tau.amegroups.com/article/view/10.21037/tau-23-432/dss>

*Peer Review File:* Available at <https://tau.amegroups.com/article/view/10.21037/tau-23-432/prf>

*Conflicts of Interest:* All authors have completed the ICMJE uniform disclosure form (available at <https://tau.amegroups.com/article/view/10.21037/tau-23-432/coif>). Z.X. is serving as an executive editor and editorial board member of *Translational Andrology and Urology* from March 2022 to February 2024. The other authors have no conflicts of interest to declare.

*Ethical Statement:* The authors are accountable for all aspects of the work in ensuring that questions related to the accuracy or integrity of any part of the work are appropriately investigated and resolved. The study was conducted in accordance with the Declaration of Helsinki (as revised in 2013). The study was approved by the Tianjin Medical University Management Committee and Ethics Committee (No. KY2021K113) and the requirement for

individual consent for this retrospective analysis was waived.

**Open Access Statement:** This is an Open Access article distributed in accordance with the Creative Commons Attribution-NonCommercial-NoDerivs 4.0 International License (CC BY-NC-ND 4.0), which permits the non-commercial replication and distribution of the article with the strict proviso that no changes or edits are made and the original work is properly cited (including links to both the formal publication through the relevant DOI and the license). See: <https://creativecommons.org/licenses/by-nc-nd/4.0/>.

## References

1. Antoni S, Ferlay J, Soerjomataram I, et al. Bladder Cancer Incidence and Mortality: A Global Overview and Recent Trends. *Eur Urol* 2017;71:96-108.
2. Tian DW, Wu ZL, Jiang LM, et al. Neural precursor cell expressed, developmentally downregulated 8 promotes tumor progression and predicts poor prognosis of patients with bladder cancer. *Cancer Sci* 2019;110:458-67.
3. Lu C, Qie Y, Liu S, et al. Selective Actionable and Druggable Protein Kinases Drive the Progression of Neuroendocrine Prostate Cancer. *DNA Cell Biol* 2018;37:758-66.
4. Madersbacher S, Hochreiter W, Burkhard F, et al. Radical cystectomy for bladder cancer today--a homogeneous series without neoadjuvant therapy. *J Clin Oncol* 2003;21:690-6.
5. Tholomier C, Souhami L, Kassouf W. Bladder-sparing protocols in the treatment of muscle-invasive bladder cancer. *Transl Androl Urol* 2020;9:2920-37.
6. International Collaboration of Trialists; Medical Research Council Advanced Bladder Cancer Working Party (now the National Cancer Research Institute Bladder Cancer Clinical Studies Group); European Organisation for Research and Treatment of Cancer Genito-Urinary Tract Cancer Group; et al. International phase III trial assessing neoadjuvant cisplatin, methotrexate, and vinblastine chemotherapy for muscle-invasive bladder cancer: long-term results of the BA06 30894 trial. *J Clin Oncol* 2011;29:2171-7.
7. Boersma LJ, van den Brink M, Bruce AM, et al. Estimation of the incidence of late bladder and rectum complications after high-dose (70-78 Gy) conformal radiotherapy for prostate cancer, using dose-volume histograms. *Int J Radiat Oncol Biol Phys* 1998;41:83-92.
8. Pettenati C, Ingersoll MA. Mechanisms of BCG immunotherapy and its outlook for bladder cancer. *Nat Rev Urol* 2018;15:615-25.
9. Ismail S, Karsenty G, Chartier-Kastler E, et al. Prevalence, management, and prognosis of bladder cancer in patients with neurogenic bladder: A systematic review. *Neurourol Urodyn* 2018;37:1386-95.
10. Alifrangis C, McGovern U, Freeman A, et al. Molecular and histopathology directed therapy for advanced bladder cancer. *Nat Rev Urol* 2019;16:465-83.
11. Ahmed M, Sottnik JL, Dancik GM, et al. An Osteopontin/CD44 Axis in RhoGDI2-Mediated Metastasis Suppression. *Cancer Cell* 2016;30:432-43.
12. Zhang N, Li F, Gao J, et al. Osteopontin accelerates the development and metastasis of bladder cancer via activating JAK1/STAT1 pathway. *Genes Genomics* 2020;42:467-75.
13. Wei R, Wong JPC, Kwok HF. Osteopontin -- a promising biomarker for cancer therapy. *J Cancer* 2017;8:2173-83.
14. Hao C, Cui Y, Owen S, et al. Human osteopontin: Potential clinical applications in cancer (Review). *Int J Mol Med* 2017;39:1327-37.
15. Arafat HA, Wein AJ, Chacko S. Osteopontin gene expression and immunolocalization in the rabbit urinary tract. *J Urol* 2002;167:746-52.
16. Wisniewski T, Zyromska A, Makarewicz R, et al. Osteopontin And Angiogenic Factors As New Biomarkers Of Prostate Cancer. *Urol J* 2019;16:134-40.
17. Pio GM, Xia Y, Piaseczny MM, et al. Soluble bone-derived osteopontin promotes migration and stem-like behavior of breast cancer cells. *PLoS One* 2017;12:e0177640.
18. Walaszek K, Lower EE, Ziolkowski P, et al. Breast cancer risk in premalignant lesions: osteopontin splice variants indicate prognosis. *Br J Cancer* 2018;119:1259-66.
19. Ostheimer C, Gunther S, Bache M, et al. Dynamics of Heat Shock Protein 70 Serum Levels As a Predictor of Clinical Response in Non-Small-Cell Lung Cancer and Correlation with the Hypoxia-Related Marker Osteopontin. *Front Immunol* 2017;8:1305.
20. Woźniak M, Pawelak A, Makuch S, et al. Osteopontin is differentially expressed in renal cell tumors. *J Histotechnol* 2020;43:90-6.
21. Sjö Dahl G, Abrahamsson J, Holmsten K, et al. Different Responses to Neoadjuvant Chemotherapy in Urothelial Carcinoma Molecular Subtypes. *Eur Urol* 2022;81:523-32.
22. Burlin AI, Tillib SV. Differentially Expressed Long Noncoding RNAs in the Promoter Region of the fork head Gene in *Drosophila melanogaster* Detected by Northern Blot Hybridization. *Mol Biol (Mosk)* 2019;53:476-84.
23. Stalke A, Pfister ED, Baumann U, et al. Homozygous

- frame shift variant in ATP7B exon 1 leads to bypass of nonsense-mediated mRNA decay and to a protein capable of copper export. *Eur J Hum Genet* 2019;27:879-87.
24. Kishi JY, Lapan SW, Beliveau BJ, et al. SABER amplifies FISH: enhanced multiplexed imaging of RNA and DNA in cells and tissues. *Nat Methods* 2019;16:533-44.
  25. Schulz D, Zanotelli VRT, Fischer JR, et al. Simultaneous Multiplexed Imaging of mRNA and Proteins with Subcellular Resolution in Breast Cancer Tissue Samples by Mass Cytometry. *Cell Syst* 2018;6:25-36.e5.
  26. Chen M, Wei L, Law CT, et al. RNA N6-methyladenosine methyltransferase-like 3 promotes liver cancer progression through YTHDF2-dependent posttranscriptional silencing of SOCS2. *Hepatology* 2018;67:2254-70.
  27. Zhen Y, Li D, Li W, et al. Reduced PDCD4 Expression Promotes Cell Growth Through PI3K/Akt Signaling in Non-Small Cell Lung Cancer. *Oncol Res* 2016;23:61-8.
  28. Tang Y, Zhang XL, Tang LJ, et al. In Situ Imaging of Individual mRNA Mutation in Single Cells Using Ligation-Mediated Branched Hybridization Chain Reaction (Ligation-bHCR). *Anal Chem* 2017;89:3445-51.
  29. Kurrasch DM, Huang J, Wilkie TM, et al. Quantitative real-time polymerase chain reaction measurement of regulators of G-protein signaling mRNA levels in mouse tissues. *Methods Enzymol* 2004;389:3-15.
  30. Zhan S, Xu H, Zhang W, et al. Sensitive fluorescent assay for copper (II) determination in aqueous solution using copper-specific ssDNA and Sybr Green I. *Talanta* 2015;142:176-82.
  31. Wang J, Teng Z, Zhang L, et al. Multifunctional Near-Infrared Fluorescent Probes with Different Ring-Structure Trigger Groups for Cell Health Monitoring and In Vivo Esterase Activity Detection. *ACS Sens* 2020;5:3264-73.
  32. Ou X, Liu Y, Zhang M, et al. Plasmonic gold nanostructures for biosensing and bioimaging. *Mikrochim Acta* 2021;188:304.
  33. Gao ZF, Ogbe AY, Sann EE, et al. Turn-on fluorescent sensor for the detection of glucose using manganese dioxide-phenol formaldehyde resin nanocomposite. *Talanta* 2018;180:12-7.
  34. Zhan S, Jiang J, Zeng Z, et al. DNA-templated coinage metal nanostructures and their applications in bioanalysis and biomedicine. *Coord Chem Rev* 2022;455:214381.
  35. Li Z, Li Y, Chang W, et al. Synthesis and Fluorescent Properties of Aminopyridines and the Application in "Click and Probing". *Molecules* 2022;27:1596.
  36. Klimek R, Wang M, McKenney VR, et al. Photo-tethered molecular beacons for superior light-induction. *Chem Commun (Camb)* 2021;57:615-8.
  37. Du J, Li Y, Yang B, et al. Allosteric DNA molecular beacons: Using a novel mechanism to develop universal biosensor arrays to fully discriminate DNA/RNA analogues. *Sens Actuator B-Chem* 2020;311:127908.
  38. Ma GM, Huo LW, Tong YX, et al. Label-free and sensitive MiRNA detection based on turn-on fluorescence of DNA-templated silver nanoclusters coupled with duplex-specific nuclease-assisted signal amplification. *Mikrochim Acta* 2021;188:355.
  39. Saady A, Varon E, Jacob A, et al. Applying styryl quinolinium fluorescent probes for imaging of ribosomal RNA in living cells. *Dyes and Pigments* 2020;174:107986.
  40. Xing C, Chen Z, Lin Y, et al. Accelerated DNA tetrahedron-based molecular beacon for efficient microRNA imaging in living cells. *Chem Commun (Camb)* 2021;57:3251-4.
  41. Kam Y, Rubinstein A, Naik S, et al. Detection of a long non-coding RNA (CCAT1) in living cells and human adenocarcinoma of colon tissues using FIT-PNA molecular beacons. *Cancer Lett* 2014;352:90-6.
  42. Tamura Y, Furukawa K, Yoshimoto R, et al. Detection of pre-mRNA splicing in vitro by an RNA-templated fluorogenic reaction. *Bioorg Med Chem Lett* 2012;22:7248-51.

**Cite this article as:** Wu Z, Wang D, Zhang Y, Zhang Z, Shen C, Xin Z, Feng Y, Hu H. SPP1 mRNA determination based on molecular beacon for the recurrence prognosis of bladder cancer. *Transl Androl Urol* 2023;12(12):1834-1844. doi: 10.21037/tau-23-432